

Optimization of Adsorption Parameters for Effective Removal of Lead (II) from Aqueous Solution

Jonas Bayuo^{1*}, Kenneth Bayetimani Pelig-Ba¹ and Moses Abdullai Abukari²

¹Department of Applied Chemistry and Biochemistry, University for Development Studies, Postal Box 24, Navrongo, Ghana

²Department of Science and Mathematics Education, University for Development Studies, Postal Box 24, Navrongo, Ghana

*Corresponding author: Jonas Bayuo, Department of Applied Chemistry and Biochemistry, University for Development Studies, Postal Box 24, Navrongo, Ghana; E-Mail: jonas87bayuo@yahoo.com

Received: December 12, 2018; Accepted: January 19, 2019; Published: March 4, 2019

Abstract

In this study, groundnut shell was used as an adsorbent to remove lead (II) ions in an aqueous solution. Response Surface Methodology (RSM) was employed for the modeling and optimization of adsorption of lead (II) ion onto groundnut shell. The effects of three adsorption variables (contact time, pH as well as initial metal ion concentration) on two response variables (removal efficiency and adsorption capacity) were investigated using Central Composite Design (CCD), which is a subset of the Response Surface Methodology. Numerical optimization applying desirability function was used to identify the optimum conditions for a maximum removal efficiency and adsorption capacity of lead (II) ions onto the groundnut shell. The optimum operating condition for the adsorption of Pb (II) was found to be contact time of 90 min, pH of 8 and initial concentration of 75 mg/L with the desirability of 0.966. The maximum removal efficiency and adsorption capacity of Pb (II) ions under this operating condition were found to be 90.26% and 3.428 mg/g respectively. The equilibrium adsorption isotherm and kinetic studies showed that Langmuir isotherm and pseudo-second-order kinetic model fitted well to the experimental data. The characterization studies were performed using Fourier Transform Infrared Spectrometer (FT-IR) and Scanning Electron Microscope (SEM).

Keywords: Adsorption; Groundnut shell; Lead; Response surface methodology; Optimization; Heavy metals

Introduction

The upsurge in industrial, agricultural, and domestic activities has led to the discharge of large amounts of wastewater containing toxic pollutants. The growing awareness of the adverse effects of the presence of these water pollutants has led to increasingly strict regulation of water pollution; hence making the treatment of wastewater generated from industrial activities a high priority [1]. Increase in industrialization and anthropogenic activities have emerged as a major problem in recent years due to the release of large amounts of heavy metals as waste directly into the surface waters, ponds, and rivers. These heavy metals disturb the ecosystem and make it unfit for human consumption [2]. Once released into the environment, these pollutants accumulate into living tissues via the food chain and cause health-related problems even at lower concentrations.

Lead is a major toxic pollutant, which finds its way into water streams through various industrial operations. Lead is a dangerous metal, even in very low concentrations that accumulate in the body causing severe damage to the central nervous

Citation: Bayuo J, Kenneth B, Moses AA. Optimization of Adsorption Parameters for Effective Removal of Lead (II) from Aqueous Solution. Phys Chem Ind J. 2019;14(1):123.

© 2019 Trade Science Inc.

system, liver, kidney and bone marrow [3]. Recent studies indicate that the rise in mortality and systolic blood pressure has its root cause from elevated blood-lead levels. High concentration of lead in the blood has been found to cause hearing impairment, intellectual impediments, and alteration of puberty in girls [4,5]. For instance, children exposed to lead suffer from impaired development, lower intelligent quotient, shortened attention span, hyperactivity and mental deterioration [6-8]. The conventional methods for treatment of heavy metals wastes include; precipitation, adsorption with activated carbon, ion exchange, membrane processes, oxidation and reduction [9]. However, most of these methods resulted in incomplete removal of metal ions, low selectivity, high operational cost, high consumption of reagents, energy, and generation of secondary pollutants [10,11]. Besides, it has been revealed that some of these techniques are usually incapable of meeting the discharged standard limits for heavy metals concentrations ranging between 0.1-3 mg/L [12]. The adsorption technique still remains the most effective and common applicable technology widely used over other techniques in global environmental protection [13]. Adsorption has distinct advantages over the conventional methods which include: reusability of biomaterial, low operating cost, selectivity for specific metal, short operation time and no chemical sludge [14,15]. Several agricultural materials including plants seeds [16-18] and orange peel [19] have been used for the adsorption of heavy metals as reported in many studies. Groundnut shells are carbonaceous, fibrous solid agricultural waste that encounters disposal problem but potentially suitable for making low-cost adsorbent for adsorption of heavy metals from water and wastewaters due to its high carbon content [20].

The application of statistical experimental design techniques in the adsorption process has been revealed to reduce process variability and require fewer resources [21]. Response Surface Methodology is a mathematical model that was reported to be a very useful tool that helped in investigating the interactive effects of process variables and in building a mathematical model, which accurately describes the overall process. Basically, it had been used in the multivariate experimental design, statistical modeling and process optimization [22].

This study explored the effect of contact time, pH and initial metal ion concentration on removal efficiency and adsorption capacity of groundnut shell as an adsorbent in the adsorption of Pb (II) ion. Response Surface Methodology via Central Composite Design was used to design the experiment, generate a model and optimize the process variables. The experimental data were analyzed by fitting to a second-order polynomial model, which was statistically validated by performing Analysis of Variance (ANOVA) and Lack-of-fit test to evaluate the significance of the model. Desirability function was also used to find the optimum conditions where the maximum removal efficiency and adsorption capacity were obtained for the removal of Pb (II) ion using groundnut shell. Moreover, equilibrium adsorption isotherm and kinetic studies were investigated.

Material and Method

Preparation of adsorbent

The collected shells were washed thoroughly by distilled water to remove dust and other impurities. It was thereafter heated up at 105 °C for 24 hours in an oven. The dried shells were crushed into smaller pieces by mortar and pestle and ground into powder with the aid of mechanical grinder. The obtained powder was sieved to a particle size less than 300 µm and used for the adsorption experiments without any kind of chemical or physical modifications [23,24].

Preparation of adsorbate

All chemicals used for the study were analytical reagent grade and all the glassware used were washed and rinsed several times. In the preparation of a stock solution of the adsorbate, Pb (II); procedures specified in [25] were followed. Specifically, a known mass (1.599 g) of lead nitrate, $[Pb(NO_3)_2]$ was dissolved in 200 mL of distilled water, then 10 mL of

concentrated HNO₃ was added and the resulting solution was diluted to the 1000 mL mark of the volumetric flask using de-ionized water. Working metal ion solutions were prepared from the stock solution containing 1000 mg/L of Pb (II) by diluting the stock solution with de-ionized water to the required concentrations. The Pb (II) concentrations were determined spectrophotometrically (Carry 60 UV-Vis Spectrophotometer) by the Dithizone method [25].

Characterization of adsorbent

The surface functional groups on groundnut shell sample before and after adsorption of Pb (II) were determined by Fourier Transform Infrared (FT-IR) spectrophotometer while scanning electron microscopy was used to determine the surface morphology, crystalline structure, and orientation of the groundnut shell sample.

Preliminary adsorption experiments

Adsorption experiments were carried out using batch technique in order to examine and evaluate variables significance on the removal efficiency (%) and adsorption capacity (mg/g) of Pb (II) by shaking 100 mL of the metal ion solutions in a 250 mL Erlenmeyer flask according to the contact time, pH as well as initial concentrations. The aqueous samples were analyzed using Carry 60 UV-Vis spectrophotometer. The removal efficiency and adsorption capacity were evaluated using the following Eq. 1 and Eq. 2 [26].

$$\text{Removal efficiency} = \left(C_0 - C_e / C_0 \right) \times 100 \quad (1)$$

$$\text{Adsorption capacity } (q_e) = \left(C_0 - C_e / m \right) \times V \quad (2)$$

Where, C_0 is the initial metal ion concentration (mg/L), C_e is the equilibrium metal ion concentration (mg/L), q_e represents the equilibrium mass of the adsorbed substance per unit mass of adsorbent, V is the volume of solution (mL), and m is the mass of the adsorbent (g).

Experimental design

Central Composite Design, a form of response surface methodology has been widely used as a statistical method based on the multivariate nonlinear model for the optimization of process variables of adsorption. The optimization process involves three major steps: performing the statistically designed experiments; estimating the coefficients in a mathematical model and, predicting the response and checking the adequacy of the model [27]. Central Composite Design is used to determine the regression model equations and operating conditions from the appropriate experiments. It is useful in studying the interactions of the various factors affecting the process [28]. The Central Composite Design was applied in this present study to determine the optimum process variables for adsorption of Pb (II) ion using groundnut shell. The central composite design was used for fitting a second-order model, which requires only a minimum number of experiments for modeling [27]. The Central Composite Design consists of 2^n factorial runs with $2n$ axial runs and n_c center runs. The center points are used to determine the experimental error and reproducibility of the data and the axial points are chosen such that they allow rotatability that ensures that the variance of the model prediction is constant at all points equidistant from the design center [29]. Therefore, according to Owolabi et al., [30], the number of experimental runs required is given by the Eq. 3.

$$N = 2^n + 2n + n_c \quad (3)$$

Where, N =Total number of experimental runs, n = number of independent variables (factors) and n_c =number of center points. Three independent variables were considered in this study, they are (i) contact time (A), (ii) pH (B) and (iii) initial metal ion concentration (C). For the independent three variables (factors), the number of experimental runs required was computed by Eq.4.

$$N = 2^n + 2n + n_c = 2^3 + 2(3) + 6 = 8 + 6 + 6 = 20 \quad (4)$$

This implied that 20 experimental runs consisting of 8 factorial runs, 6 axial runs and 6 center runs were required for the modeling and optimization of the adsorption variables.

Development of regression models equations

Each response (removal efficiency and adsorption capacity) was used to develop an empirical model that correlate the response to the three factors that is, contact time (A), pH (B) and initial metal ion concentration (C) using second-order polynomial equation [31] given by Eq. 5.

$$Y = b_0 + \sum_{i=1}^n b_i X_i + \sum_{i=1}^n b_{ii} X_i^2 + \sum_{i=1}^{n-1} \sum_{j=i+1}^n b_{ij} X_i X_j \quad (5)$$

Where Y is the predicted response, b_0 is the constant coefficient, b_i is the linear coefficient, b_{ij} is the interaction coefficient, b_{ii} is the quadratic coefficient, X_i and X_j are the coded values for the factors.

Statistical analysis

The significance of the model equations and their terms were evaluated using statistical tools such as coefficient of determination (R-squared), Fisher value (F-value), probability (p-value), and residual [32].

Optimization of the adsorption process

In order to obtain the maximum response that jointly satisfies all process conditions, optimization was carried out using the Design Expert software under RSM. In numerical optimization, we chose the desired goal for each factor and response. The goal was to maximize (for responses only) and set to an exact value (factors only). A minimum and a maximum level must be provided for each parameter included. A weight can be assigned to each goal to adjust the shape of its particular desirability function. The goals are combined into an overall desirability function. Desirability is an objective function that ranges from zero outside of the limits, to one at the goal. The goal seeking begins at a random starting point and proceeds up the steepest slope to a maximum. There may be two or more maxima because of curvature in the response surfaces and their combination in the desirability function. Starting from several points in the design space improves the chances of finding the 'best' local maximum [33]. In the optimization analysis, the target criterion was set as maximum values for the three independent variables, (A-Contact time, B-pH and C-Initial concentration) and two dependent variables (removal efficiency and adsorption capacity) for the adsorption of Pb (II) ion as summarized in **TABLE 1**.

Models validation

The models were validated by conducting a batch experiment under optimum operating conditions to compare the experimental values with predicted values under optimum operating condition.

TABLE 1. Constraints set for all factors and responses for the adsorption of Pb (II) ion.

Name	Goal	Lower Limit	Upper Limit	Lower Weight	Upper Weight	Importance
A:Contact time	maximize	60	90	1	1	3
B:pH	maximize	6	8	1	1	3
C:Initial concentration	maximize	25	75	1	1	3
Removal efficiency	maximize	30.86	97.20	1	1	3
Adsorption capacity	maximize	0.123	3.645	1	1	3

Equilibrium adsorption isotherm studies

In this study, the applicability of two-parameter isotherm models [34,35] was tested in order to choose the most appropriate model that would best describe and predict the adsorption of Pb (II) onto groundnut shell.

Langmuir isotherm model

Langmuir model was initially developed to describe the gas-solid phase adsorption onto activated carbon [36,37]. It is an empirical model that assumes that adsorption can only occur at a finite number of definitely localized sites and the adsorbed layer is one molecule in thickness or monolayer adsorption. In its formulation, Langmuir model denotes homogeneous adsorption with no transmigration of the solute in the plane to the surface of the solid. The Langmuir adsorption isotherm model has the following assumptions:

- 1 Monolayer adsorption (the adsorbed layer is one molecule thick)
- 2 Adsorption occurs at specific homogeneous sites of the adsorbent and all adsorption sites are identical and energetically equivalent
- 3 Once a molecule occupies an adsorption site, no further adsorption occurs on that site.

The non-linear and linear expressions of Langmuir isotherm are given in Eq. 6 and Eq. 7 [34].

$$q_e = q_m K_L \frac{C_e}{1 + K_L C_e} \quad (6)$$

$$\frac{C_e}{q_e} = \frac{1}{q_m K_L} + \frac{C_e}{q_m} \quad (7)$$

where, q_e is the corresponding adsorption capacity (mg/g), C_e is the concentration at equilibrium (mg/L); K_L (L/mg) and q_m (mg/g) are constants which are linked to the net enthalpy of adsorption and adsorption capacity respectively. The constants K_L and q_m can be obtained from Eq. 7 by plotting $\frac{C_e}{q_e}$ versus C_e with a slope of $\frac{C_e}{q_m}$ and intercept of $\frac{1}{q_m K_L}$. The fitness of an adsorption process to Langmuir isotherm model is generally determined using Eq. 8. The values of R_L give an idea about the shape of isotherm [38].

$$R_L = \frac{1}{1 + K_L C_0} \quad (8)$$

where, R_L is the separation factor, C_0 is the initial metal ions concentration and K_L is the Langmuir constant (L/mg) which is related to the energy of adsorption through the Arrhenius equation **TABLE 2**.

TABLE 2. The ranges of R_L values for comparison.

R_L	Shape of Isotherm
$R_L > 1$	Unfavorable
$R_L = 1$	Linear
$0 < R_L < 1$	Favorable
$R_L = 0$	Irreversible

Freundlich isotherm model

The Freundlich model is the earliest well-known expression relating non-ideal and reversible adsorption that is not limited to the formation of the monolayer. Hence, this empirical model is applicable to multilayer adsorption with non-uniform distribution of adsorption heat and affinities over the heterogeneous surface of the solid [35,39]. The Freundlich expression is an exponential equation and non-linear and linear expressions of the Freundlich isotherm model can be illustrated by Eq. 9 and Eq. 10 [35].

$$q_e = K_F C_e^{\frac{1}{n}} \quad (9)$$

$$\log q_e = \log K_F + \frac{1}{n} \log C_e \quad (10)$$

where, q_e is the corresponding adsorption capacity (mg/g), C_e is the concentration of solute in the bulk solution at equilibrium (mg/L); K_F is a constant indicative of the relative adsorption capacity of the adsorbent (mg/g) and n is a constant indicative of the intensity of adsorption. From the plot of $\log q_e$ versus $\log C_e$ in Eq. 10, the constants K_F can be obtained from the intercept of $\log K_F$ and n from the slope of $\frac{1}{n}$. The adsorption intensity or surface heterogeneity is measured from the slope ranging between 0 and 1; and the surface becomes more heterogeneous as its value gets closer to zero. While a value of $\frac{1}{n}$ below unity indicates chemical adsorption, a value $\frac{1}{n}$ above one implies cooperative adsorption [40,41].

Equilibrium adsorption kinetic studies

Adsorption kinetics study is necessary since it provides information about the mechanisms of adsorption and the rates that are essential for the efficacy of the process. Adsorption is a time-dependent process and contact time from experimental results can be used to study the rate-limiting step in the adsorption process in terms of the kinetic energy [42]. Lagergren's first order equation and Ho's second order equation are such examples of kinetics models commonly used to describe these adsorption kinetic models [43]. During the removal of contaminants from wastewater, it is important to know the rate of adsorption to optimize the design parameters [44]. This is due to the fact kinetics of the system controls the adsorbate residence time and reactions dimensions. Hence, predicting the rate at which adsorption processes take place for a particular system is probably the most important key in designing adsorption systems [44,45].

Pseudo-first-order rate equation

Lagergren, [46] used a first-order rate equation to describe the kinetics of the adsorption process of oxalic acid and malonic acid onto charcoal. It was the earliest model relating to the adsorption rate based on the adsorption capacity and can be presented by Eq. 11.

$$\frac{dq_t}{dt} = k_{p1}(q_e - q_t) \quad (11)$$

where, k_{p1} (min^{-1}) is the pseudo-first-order rate constant, q_e and q_t (mg/g) are the adsorption capacities at equilibrium and time t (min) respectively. Integrating Eq. 11 with the boundary conditions of $q_t = 0$ at $t = 0$ and $q_t = q_t$ at $t = t$ yields Eq. 12.

$$\log\left(\frac{q_e}{q_e - q_t}\right) = k_{p1} t \quad (12)$$

Equation (12) can be reorganized as:

$$\log(q_e - q_t) = \log q_e - \frac{k_{p1}}{2.303} t \quad (13)$$

In recent years, Lagergren's first order rate equation commonly called pseudo-first-order has been used globally to describe the adsorption mechanisms of pollutants from aqueous media in different fields. For instance, the removal of methylene blue onto broad bean peels from aqueous solution and malachite green removal from aqueous solutions by oil palm trunk fiber [19,47,48]. The equilibrium sorption capacity (q_e) and the pseudo-first order rate constant (k_{p1}) can be determined experimentally from slope and intercept of plotting of $\log(q_e - q_t)$ versus t from Eq. 13.

Pseudo-second-order rate equation

Similarly, Ho, [44] second-order rate equation is well-known as the pseudo-second-order rate equation to differentiate kinetic of adsorption based on adsorption capacity from the concentration of the solution. This kinetic equation has been used effectively for the removal of dyes, herbicides, oils, metal ions, and organic substances from water and wastewaters [49-52].

The integrated form of pseudo-second-order is by Eq. 14.

$$\frac{dq_t}{dt} = k_{p2}(q_e - q_t)^2 \quad (14)$$

Equation (14) can be written as given by Eq. 15.

$$\frac{dq_t}{(q_e - q_t)^2} = k_{p2} dt \quad (15)$$

Integrating Eq. 15 with the boundary conditions of $q_t = 0$ at $t = 0$ and $q_t = q_t$ at $t = t$, yields Eq. 16.

$$\frac{1}{(q_e - q_t)} = \frac{1}{q_e} + k_{p2} t \quad (16)$$

Hence, Eq. 16 can be rearranged as follows:

$$\frac{t}{q_t} = \frac{1}{k_{p2} q_e^2} + \frac{1}{q_e} t \quad (17)$$

The pseudo-second-order rate constant (k_{p2}) and the equilibrium adsorption capacity (q_e) can be obtained from the slope and intercept by plotting $\frac{t}{q_t}$ vs t from Eq. 17.

Results and Discussion

Characterization of the adsorbent

Fourier Transform Infrared (FT-IR) spectrophotometer and Scanning Electron Microscopy (SEM) were used in the characterization of the groundnut shell as an adsorbent.

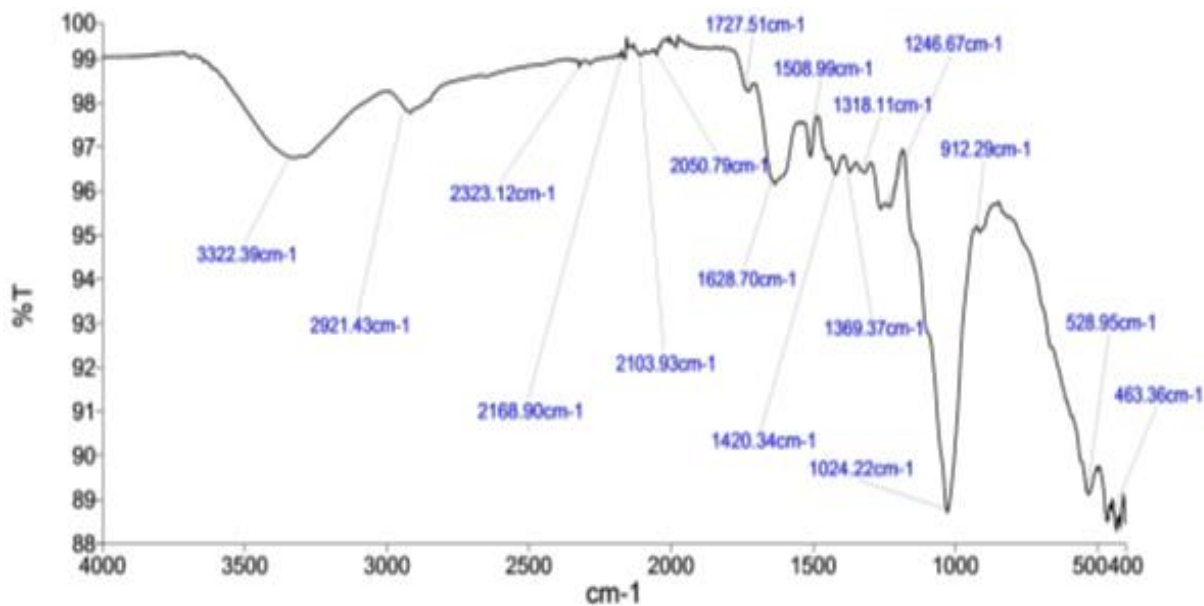
TABLE 3. FT-IR spectral characteristics of groundnut shell before and after Pb (II) ions adsorption.

Functional groups of IR absorption bands	Wave number, cm ⁻¹		
	Before adsorption of Pb (II) ion	After adsorption of Pb (II) ion	Shift differences
	Absorption bands		
O-H	3322.39	3319.01	3.38
N-H			
C-H	2921.43	2892.26	29.17
C≡C	2323.12	2323.20	0.08
	2168.90	2168.90	0.00
	2103.93	2103.93	0.00
	2050.79	2050.79	0.00
C=O	1727.51	1729.34	1.83
	1628.70	1621.91	6.79
C=C	1246.67	1246.00	0.67
C-O	1024.22	1421.12	2.72

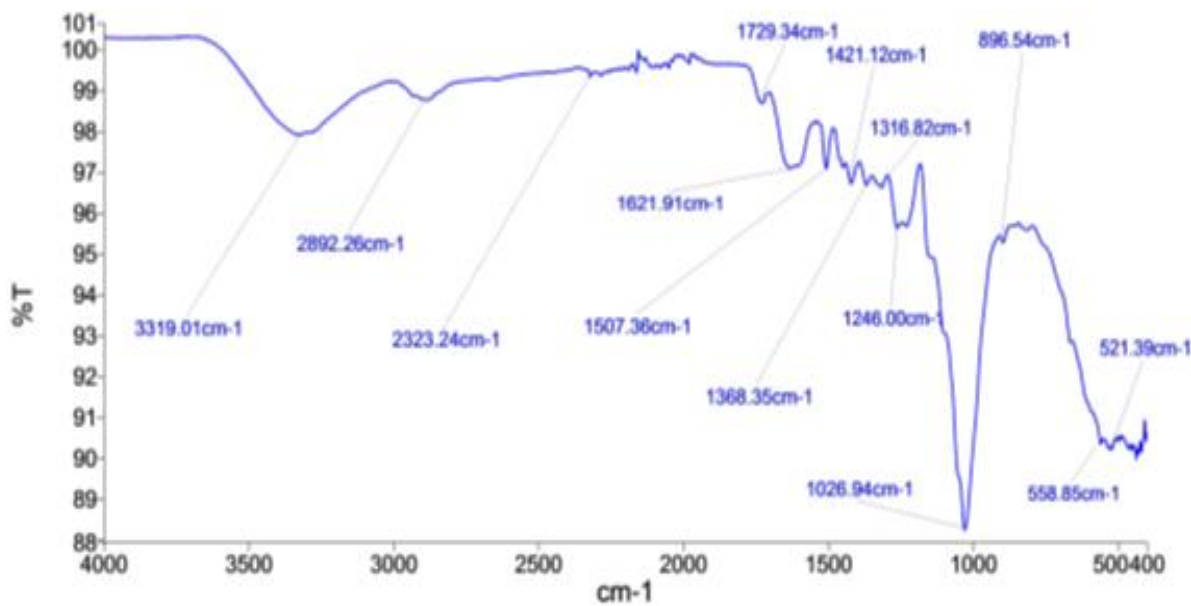
FT-IR analysis of the groundnut shell

In order to evaluate the mechanism of the adsorption of Pb (II) and identify the functional groups present on the surface of the groundnut shell, the FT-IR analysis was performed. The distinct absorption bands in the raw groundnut sample before (FIG. 1a) the adsorption process are presented in TABLE 3 which corresponded to O-H₂, N-H₂, C-H₂, C=O, C=C, and C-O stretching vibrations respectively.

These absorption bands (TABLE 3) were shifted after using the sample to adsorbed Pb (II) ions as shown in FIG. 1b. It was found that the absorption bands at 2323.12, 1727.51 and 1024.22 cm⁻¹ were shifted to higher wavenumbers while the absorption bands at 3322.39, 2921.43, 1628.90 and, 1246.67 cm⁻¹ were shifted to lower wavenumbers. The C≡C stretching vibration was located at absorption bands 2323.12, 2168.90, 2103.93 and 2050.79 cm⁻¹ respectively as shown in FIG. 1a. These absorption bands showed the same signals after the sample was used to adsorbed Pb (II) ions (FIG. 1b). However, it was observed that the absorption band at 2323.12 cm⁻¹ shifted to 2323.24 cm⁻¹. Moreover, the adsorption intensity for the N-H bending vibration at 1508.99 cm⁻¹ (FIG. 1a) shifted to 1507.36 cm⁻¹ (FIG. 1b) after and Pb (II) uptake. The change in absorption intensity and the shift in wavenumber of functional groups showed that these functional groups were responsible for the effective performance of the groundnut shell during the adsorption process [53]. In this case, the Pb (II) ions are bound to the active sites of the adsorbent through either electrostatic attraction or complexation mechanism.



(a)



(b)

FIG. 1. FT-IR spectra of groundnut shell (a) before treatment with Pb (II) ions (b) after treatment with Pb (II) ions.

Scanning electron microscope analysis of the adsorbent

The surface morphology of the groundnut shells sample before and after the adsorption process was examined by SEM analysis, and the results are depicted in FIG. 2. FIG. 2a shows the SEM image of groundnut shells sample without Pb (II). The image revealed various pores on the surface of the sample studied which indicated a good possibility for Pb (II) to be

adsorbed. However, the SEM image of groundnut shells samples loaded with Pb (II) shown in **FIG. 2b** revealed that those pores earlier seen on the fresh adsorbent have been blocked due to adsorption of Pb (II) onto its surface.

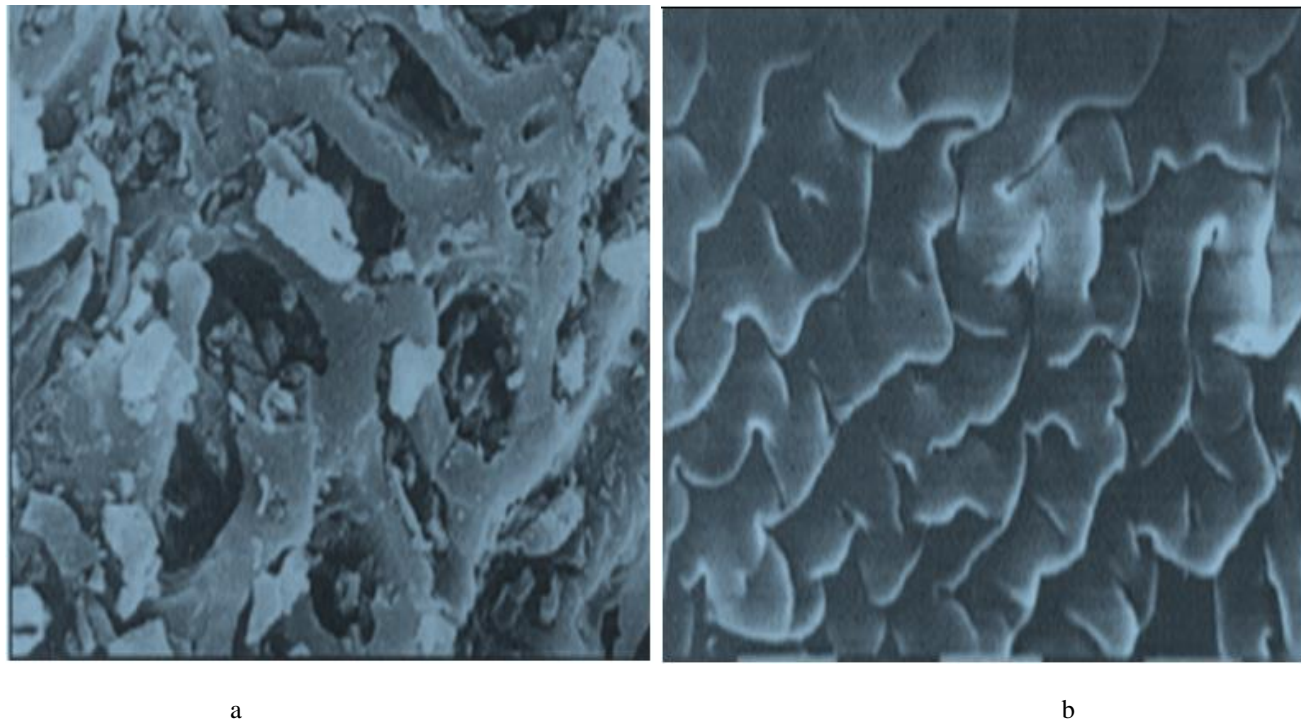


FIG. 2. SEM micrograph of groundnut shell (a): before adsorption of Pb, (b): after the adsorption of Pb (II).

Development of regression model equations using CCD

The complete design matrix of the factors, their ranges (in terms of coded and uncoded points) and their corresponding responses values for the removal efficiency (Y1) and adsorption capacity (Y2) are presented in **TABLE 4**. The highest and lowest removal efficiency (Y1) of Pb (II) was found to be 97.20 % and 30.86 % respectively. In terms of adsorption capacity (Y2), the highest and lowest adsorption capacity (Y2) was found to be 3.645 mg/g and 0.123 mg/g respectively.

The model summary statistics (**TABLES 5 and 6**) showed that the quadratic models of the responses were selected as suggested by the software because the additional terms were significant and the models were not aliased [54]. The quadratic models for the responses, Y1 and Y2 were not aliased implying that the quadratic models could be employed to describe the relationship between responses Y1 and Y2 and the interacting variables (factors).

TABLE 4. Design matrix of Pb (II) adsorption factors and their respective responses from the experiment.

Run	Space Type	Coded factors			Uncoded factors			Y 1	Y 2
		A (min)	B	C (mg/L)	A (min)	B	C (mg/L)	Removal efficiency (%)	Adsorption capacity (mg/g)
1	Center	0.000	0.000	0.000	75.0	7.0	50.0	32.80	0.820
2	Factorial	1.000	1.000	-1.000	90.0	8.0	25.0	64.40	0.805
3	Factorial	-1.000	-1.000	1.000	60.0	6.0	75.0	78.93	2.960
4	Factorial	-1.000	1.000	1.000	60.0	8.0	75.0	85.60	3.210
5	Factorial	-1.000	1.000	-1.000	60.0	8.0	25.0	92.80	1.160
6	Factorial	1.000	-1.000	-1.000	90.0	6.0	25.0	41.20	0.515
7	Center	0.000	0.000	0.000	75.0	7.0	50.0	34.80	0.870
8	Factorial	1.000	-1.000	1.000	90.0	6.0	75.0	78.53	2.945
9	Center	0.000	0.000	0.000	75.0	7.0	50.0	47.60	1.190
10	Center	0.000	0.000	0.000	75.0	7.0	50.0	45.40	1.135
11	Factorial	-1.000	-1.000	-1.000	60.0	6.0	25.0	38.00	0.475
12	Factorial	1.000	1.000	1.000	90.0	8.0	75.0	97.20	3.645
13	Center	0.000	0.000	0.000	75.0	7.0	50.0	51.00	1.275
14	Axial	0.000	-1.682	0.000	75.0	5.3	50.0	68.40	1.710
15	Axial	1.682	0.000	0.000	100.2	7.0	50.0	68.80	1.720
16	Axial	0.000	0.000	1.682	75.0	7.0	92.1	78.16	3.597
17	Axial	0.000	0.000	-1.682	75.0	7.0	8.0	30.86	0.123
18	Axial	-1.682	0.000	0.000	49.8	7.0	50.0	73.40	1.835
19	Axial	0.000	1.682	0.000	75.0	8.7	50.0	96.80	2.420
20	Center	0.000	0.000	0.000	75.0	7.0	50.0	52.80	1.320

TABLE 5. Model summary statistics for removal efficiency (response Y1).

Source	Std. Dev.	R ²	Adjusted R ²	Predicted R ²	PRESS	Comment
Linear	18.28	0.4541	0.3449	0.0728	8513.88	
2FI	19.26	0.5151	0.2727	-0.771	16261.72	
Quadratic	8.4	0.9309	0.8618	0.7207	4400.66	Suggested
Cubic	8.08	0.9645	0.8721	-12.7494	1.26E+05	Aliased

TABLE 6. Model summary statistics for adsorption capacity (response Y2).

Source	Std. Dev.	R ²	Adjusted R ²	Predicted R ²	PRESS	Comment
Linear	0.4823	0.8423	0.8108	0.7553	5.42	
2FI	0.534	0.8454	0.7681	0.431	12.59	
Quadratic	0.2157	0.9811	0.9622	0.8659	2.97	Suggested
Cubic	0.198	0.9911	0.9681	-2.2837	72.68	Aliased

TABLE 5 (response Y1) showed that the quadratic model had a small standard deviation of 8.40 and high R² (0.9309) with predicted R² (0.7207) that is in reasonable agreement with adjusted R² (0.8618). Whilst, in TABLE 6 (response Y2), the quadratic model had a small standard deviation of 0.2157, high R² (0.9811), predicted R² (0.8659) and adjusted R² (0.9622).

The R^2 values of both responses were close to unity with smaller standard deviations indicating the suitability of the model in predicting the responses [55]. However, a large value of R^2 as posited by [30] does not always imply that the regression model is a good one and such inference can only be made based on a similarly high value of adjusted R^2 . For the regression model to be in good agreement, the adjusted R^2 and predicted R^2 should be within 20% [56]. This requirement was satisfied in this study because the difference between the values of the adjusted R^2 and predicted R^2 for both responses were within 20%. This confirmed that the model for each response is highly significant and indicated a good agreement between the experimental and predicted values of the removal efficiency and adsorption capacity.

TABLES 7 and 8 showed that the adequate precisions of both responses were greater than 4.0 which implies that the models were in good agreement and highly significant. The Predicted R^2 values of 0.7207 and 0.8659 for responses Y1 and Y2 respectively showed that the models were adequate and offer 72.07% and 86.59% variability in prediction removal efficiency and adsorption capacity beyond the experimental range of process conditions during the adsorption of Pb (II) ion. The R^2 values of 0.9309 and 0.9811 also implied that 93.09% and 98.11% of the variation in removal efficiency and adsorption capacity respectively could be attributed to the three factors considered.

TABLE 7. Fit Statistics for removal efficiency (response Y1).

Std. Dev.	8.4	R²	0.9309
Mean	62.87	Adjusted R ²	0.8618
C.V. %	13.35	Predicted R ²	0.7207
		Adequate Precision	11.1266

TABLE 8. Fit Statistics for adsorption capacity (response Y2).

Std. Dev.	0.2157	R²	0.9811
Mean	1.69	Adjusted R ²	0.9622
C.V.%	12.79	Predicted R ²	0.8659
		Adeq Precision	24.0982

The results in **TABLE 9** showed that the quadratic models were selected as suggested by the software and Eq. 18 and Eq. 19 gave the response surface model equations in their coded values.

$$Y1 = +44.36 - 1.59 A + 11.06 B + 13.43 C - 2.45 AB + 4.55 AC - 6.58 BC + 9.76 A^2 + 13.82 B^2 + 3.89 C^2 \quad (18)$$

$$Y2 = +1.110 - 0.0065 A + 0.2284 B + 1.150 C + 0.0069 AB + 0.0919 AC - 0.0031 BC + 0.2410 A^2 + 0.3426 B^2 + 0.2701 C^2 \quad (19)$$

TABLE 9. Final equations in terms of coded factors for removal efficiency and adsorption capacity.

Removal efficiency (Y1)	=	Adsorption capacity (Y2)	=
+44.36		+1.1100	
-1.59	A	-0.0065	A
+11.06	B	+0.2284	B
+13.43	C	+1.1500	C
-2.45	AB	+0.0069	AB
+4.55	AC	+0.0919	AC
-6.58	BC	-0.0031	BC
+9.76	A ²	+0.2410	A ²
+13.82	B ²	+0.3426	B ²
+3.89	C ²	+0.2701	C ²

In the response Y1 model Eq. 18, the factors that have a positive effect on the removal efficiency of Pb (II) are C, AC, A², B² and C². Whilst in response Y2 model Eq. 19, factors AB, AC, A², B² and C² have a positive effect on the adsorption capacity for the adsorption of Pb (II). The negative values in both responses (Y1 and Y2) model equations indicated an inverse relationship and positive values favored the optimization of the process conditions.

Statistical and graphical analysis

The model equations selected for removal efficiency (response Y1) and adsorption capacity (response Y1) were further analyzed using ANOVA component of the software to validate the importance and the adequacy of the models. In TABLES 10 and 11, the model terms for both responses (Y1 and Y2) have p-values less than 0.05 and F-values of 13.47 and 51.88 respectively.

TABLE 10. ANOVA for Quadratic model for removal efficiency (response Y1).

Source	Sum of Squares	df	Mean Square	F-value	p-value	Comment
Block	61.84	1	61.84			
Model	8547.57	9	949.73	13.47	0.0003	significant
A-Contact time	34.60	1	34.60	0.4908	0.5013	
B-pH	1671.69	1	1671.69	23.71	0.0009	significant
C-Initial concentration	2463.33	1	2463.33	34.94	0.0002	significant
AB	48.02	1	48.02	0.6812	0.4305	
AC	165.62	1	165.62	2.35	0.1597	
BC	346.72	1	346.72	4.92	0.0538	
A ²	1371.35	1	1371.35	19.45	0.0017	significant
B ²	2752.12	1	2752.12	39.04	0.0001	significant
C ²	218.38	1	218.38	3.1	0.1122	
Residual	634.43	9	70.49			
Lack of Fit	467.10	5	93.42			Not significant
Pure Error	167.33	4	41.83			
Cor Total	9243.84	19				

TABLE 11. ANOVA for Quadratic model for adsorption capacity (response Y2).

Source	Sum of Squares	df	Mean Square	F-value	p-value	Comment
Block	0.0538	1	0.0538			
Model	21.71	9	2.41	51.88	<0.0001	significant
A-Contact time	0.0006	1	0.0006	0.0123	0.9141	
B-pH	0.7124	1	0.7124	15.32	0.0035	significant
C-Initial concentration	17.93	1	17.93	385.55	<0.0001	significant
AB	0.0004	1	0.0004	0.0081	0.9301	
AC	0.0675	1	0.0675	1.45	0.2589	
BC	0.0001	1	0.0001	0.0017	0.9682	
A ²	0.8362	1	0.8362	17.98	0.0022	significant
B ²	1.69	1	1.69	36.35	0.0002	significant
C ²	1.05	1	1.05	22.6	0.001	significant
Residual	0.4186	9	0.0465			
Lack of Fit	0.314	5	0.0628	2.4	0.2082	Not significant
Pure Error	0.1046	4	0.0261			
Cor Total	22.19	19				

The $p < 0.05$ implied that the models were highly significant and higher F-values indicated that the model terms have the most significant effect on the response function.

The significant model terms in response surface quadratic model for removal efficiency (response Y1) were found to be B, C, A² and B² and the model term which has the most significant effect on the response is B² with F-value of 39.04. The effect of the model terms are in the order B² > C > B > A². The response surface quadratic model for adsorption capacity (response Y2) was found to have C, A², B² and C² as the significant model terms. The model term having the most significant effect on the response is C with F-value of 385.55 and the effect is in the order C > B² > C² > A² > B. It was observed that, the lack of fit F-values of responses Y1 and Y2 were not significant as the p-values were >0.05 indicating that the models were valid.

Interaction of factors

The interactions between three independent variables (A-Contact time, B-pH and C-initial concentration) and two dependent variables (Y1-removal efficiency and Y2-adsorption capacity) were studied. The actual versus predicted values of response Y1 and Y2 of Pb (II) ion were plotted. **FIG. 3** showed a minimal divergence of points from the diagonal indicating that these response surface model equations can be used to adequately represent the interaction of the three factors.

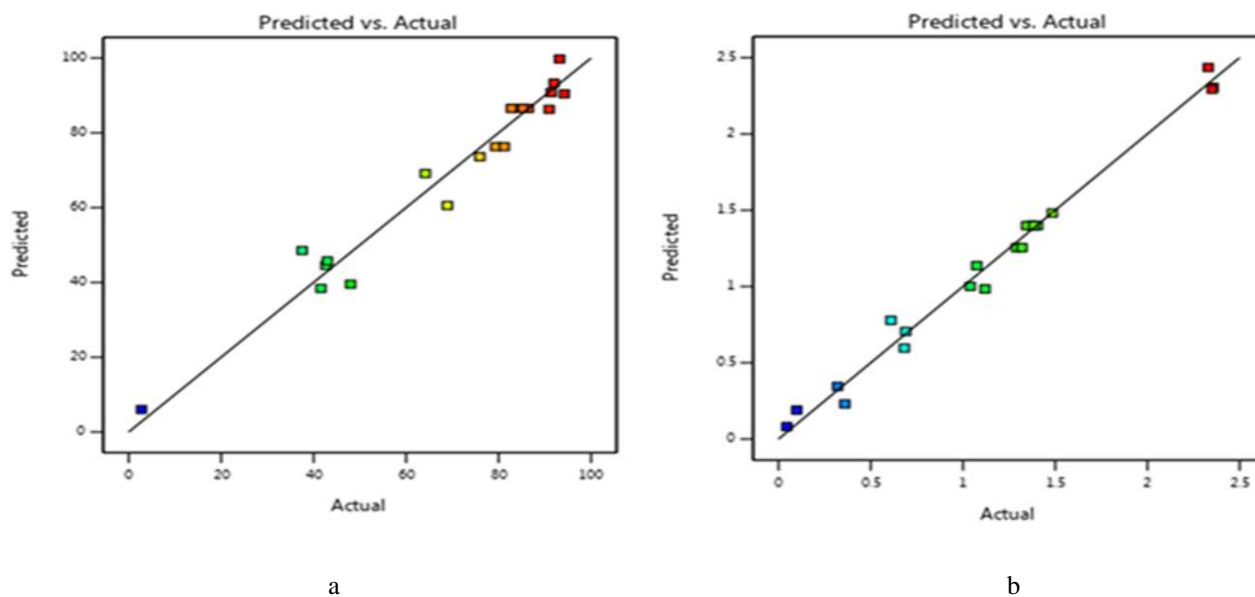


FIG. 3. Predicted versus actual values of response (a) Y1 (b) Y2.

Optimization of the adsorption process

Optimization of the two responses under the same condition was difficult because the interest regions of factors were different. When Y1 increases, Y2 decreases, and vice versa. Therefore, the function of desirability was applied using Design Expert Software (DES) version 11.0 (Stat-Ease) and the operating condition with the highest desirability was considered as selected by the software. The experimental condition with the highest desirability was selected and verified to optimize the adsorption process of Pb (II) ion (FIG. 4). The optimum operating conditions for the adsorption of Pb (II) using groundnut shell were; A-Contact time=90 min, B-pH=8 and C-Initial concentration=75 mg/L with the desirability of 0.966 after seeking 53 solutions (TABLE 12) to optimize operating conditions for Pb (II) adsorption. The removal efficiency and adsorption capacity of Pb (II) under this operating condition were found to be 90.26% and 3.428 mg/g respectively.

TABLE 12. 53 Solutions for optimization of Pb (II) ion.

Number	Contact time	pH	Initial concentration	Removal efficiency	Adsorption capacity	Desirability	
1	90.000	8.000	75.000	90.256	3.428	0.966	Selected
2	89.884	8.000	74.998	90.100	3.423	0.964	
3	90.000	7.992	75.000	90.012	3.420	0.964	
4	89.796	8.000	75.000	89.985	3.420	0.963	
5	90.000	8.000	74.734	90.052	3.409	0.963	
6	89.676	8.000	75.000	89.829	3.415	0.962	
7	90.000	7.979	75.000	89.631	3.408	0.961	
8	89.514	8.000	75.000	89.616	3.409	0.959	
9	90.000	8.000	74.376	89.779	3.384	0.959	
10	90.000	8.000	74.375	89.779	3.384	0.959	
11	90.000	7.969	74.999	89.36	3.400	0.958	
12	90.000	7.981	74.607	89.408	3.383	0.957	
13	90.000	8.000	74.132	89.595	3.366	0.957	
14	89.273	8.000	75.000	89.308	3.400	0.956	
15	89.086	8.000	75.000	89.072	3.394	0.954	
16	90.000	8.000	73.839	89.374	3.346	0.954	
17	88.874	8.000	75.000	88.803	3.386	0.951	
18	90.000	7.937	75.000	88.432	3.371	0.950	
19	89.998	8.000	73.369	89.018	3.313	0.949	
20	88.799	8.000	74.727	88.511	3.364	0.947	
21	88.478	8.000	74.996	88.321	3.372	0.946	
22	90.000	8.000	73.103	88.823	3.295	0.946	
23	88.282	8.000	75.000	88.091	3.365	0.944	
24	90.000	7.909	75.000	87.666	3.347	0.944	
25	90.000	8.000	72.770	88.576	3.272	0.942	
26	90.000	7.896	74.999	87.305	3.336	0.940	
27	90.000	8.000	72.570	88.428	3.258	0.940	
28	90.000	7.887	75.000	87.081	3.329	0.938	
29	87.789	8.000	75.000	87.516	3.348	0.938	
30	90.000	7.874	75.000	86.737	3.318	0.935	
31	87.485	8.000	75.000	87.170	3.338	0.934	
32	90.000	8.000	71.913	87.947	3.213	0.933	
33	90.000	7.862	75.000	86.418	3.307	0.932	
34	87.297	8.000	75.000	86.964	3.332	0.931	
35	90.000	7.849	75.000	86.089	3.297	0.929	
36	90.000	8.000	70.971	87.265	3.149	0.923	
37	90.000	7.816	75.000	85.262	3.271	0.922	
38	89.992	7.757	75.000	83.86	3.225	0.908	
39	90.000	8.000	68.806	85.742	3.005	0.901	
40	90.000	7.712	75.000	82.86	3.192	0.898	
41	90.000	8.000	68.099	85.255	2.958	0.893	
42	83.536	8.000	75.000	83.438	3.225	0.887	
43	90.000	7.560	75.000	79.866	3.09	0.865	
44	81.385	8.000	75.000	81.974	3.177	0.862	
45	89.999	8.000	64.428	82.839	2.725	0.855	
46	90.000	7.998	63.108	81.958	2.643	0.841	
47	90.000	8.000	61.842	81.237	2.568	0.828	
48	77.395	8.000	75.000	80.319	3.115	0.818	
49	90.000	7.250	75.000	75.769	2.932	0.805	
50	71.896	8.000	75.000	80.302	3.086	0.757	
51	90.000	6.902	75.000	74.335	2.834	0.744	
52	69.583	8.000	75.000	81.078	3.093	0.728	
53	65.875	8.000	74.999	83.291	3.128	0.667	

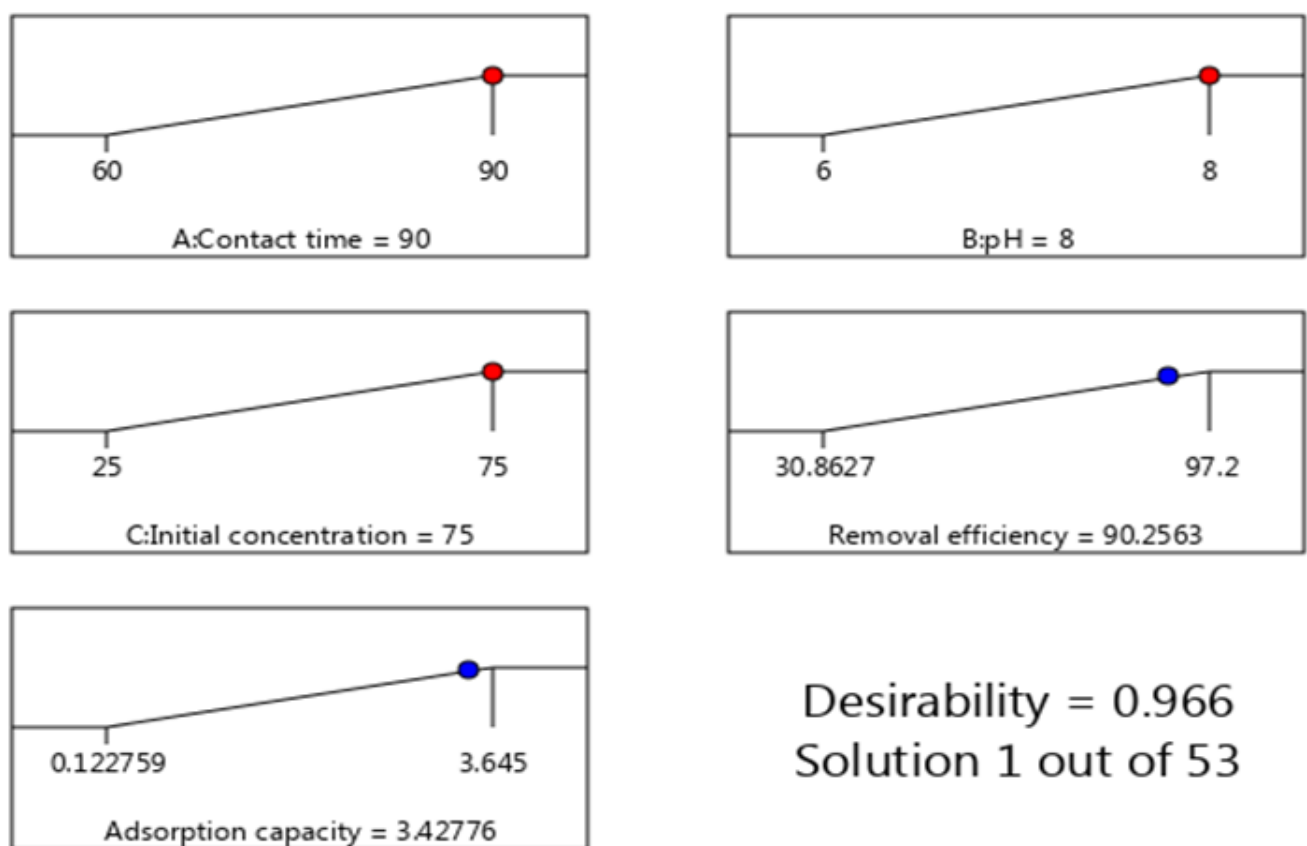


FIG. 3. Desirability ramps for Pb (II) ion.

Model validation

TABLE 13 compared the results of predicted values with observed values under optimum operating condition. The Standard Error (SE) means of predicted against observed value for removal efficiency and adsorption capacity of Pb (II) ion was found to be 6.88 and 0.18 respectively. Furthermore, the confirmation of the predicted results (TABLE 14) showed that the Standard Error Prediction (SE Pred) of removal efficiency and adsorption capacity were found to be 7.30 and 0.18 respectively. These results showed that the models and optimum operating condition developed for the factors were valid and applicable in predicting the response variables.

TABLE 13. Point Prediction and observed values of Pb (II) ion.

Run 12 Response	Predicted Mean	Predicted Median	Observed	Std Dev	SE Mean	95% CI low for Mean	95% CI high for Mean	95% TI low for 99% Pop	95% TI high for 99% Pop
Removal efficiency	90.2563	90.25630	97.200	8.395980	6.878880	74.69520	105.817	42.0665	138.44600
Adsorption capacity	3.42776	3.42776	3.645	0.215652	0.176685	3.02807	3.82745	2.19000	4.66553

TABLE 14. Confirmation of prediction for Pb (II) ion.

Run 12 Response	Predicted Mean	Predicted Median	Observed	Std Dev	n	SE Pred	95% PI low	95% PI high
Removal efficiency	90.25630	90.25630	97.200	8.395980	12	7.293380	73.75750	106.75500
Adsorption capacity	3.42776	3.42776	3.645	0.215652	12	0.187332	3.00399	3.85154

Adsorption equilibrium isotherm studies

The equilibrium isotherm experiments were carried out using 2.0 g/L of groundnut shell (optimized dose) at initial Pb (II) concentration of 15, 25, 50, 75, and 100 mg/L under room temperature (25 °C). The solutions were adjusted to pH of 6.0 using 0.1M NaOH or 0.1M HCl. The adsorbate-adsorbent solutions were agitated at a constant speed of 120 rpm for equilibrium time of 120 min.

The equilibrium data obtained from the experiments were used to analyze two-parameter adsorption isotherm models (Langmuir and Freundlich models) and the results of their linear regressions were used to find the model with the best fit. The linear plots of the adsorption isotherm models are shown in **FIG. 5 and 6** while the calculated values of their constants and correlation coefficients (R^2) are summarized in **TABLE 15**.

TABLE 15. Calculated values of the isotherm model constants and their correlation coefficients (R^2) for the adsorption of Pb (II) ions onto groundnut shell.

Langmuir				Freundlich			
q_m (mg/g)	K_L (L/mg)	R_L	R^2	K_F (mg/g)	n	1/n	R^2
4.264	0.062	0.295	0.9554	0.358	1.631	0.613	0.9098

From **FIG. 5**, the correlation coefficient (R^2) of 0.9554 showed that the Langmuir isotherm model fitted the equilibrium data well. The agreement of the Langmuir model to the equilibrium data could indicate monolayer adsorption by the groundnut shell surface that could contain a finite number of identical sites. **TABLE 15** showed that the R_L value was between 0 and 1, which indicated that the adsorption process was favorable under the studied conditions. The monolayer adsorption capacity (q_m) values were found to be 4.264 mg/g indicating high the adsorption capacity of the groundnut shell. The values of K_L were relatively high implying high surface energy in the process and consequently high bonding between metal ions and the groundnut shell.

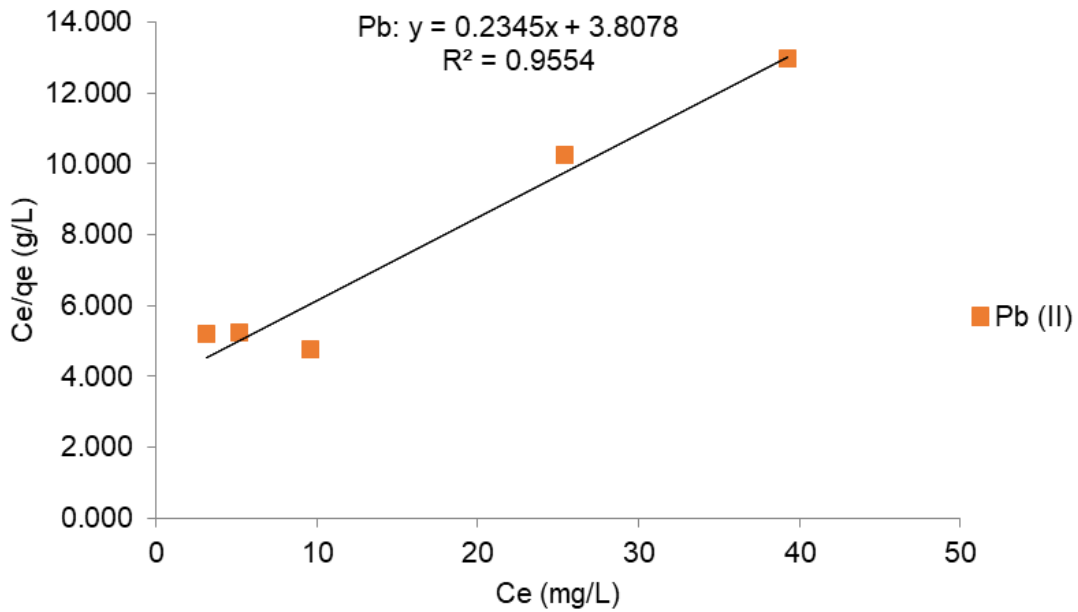


FIG. 4. Langmuir isotherm plot of Pb (II) ion onto groundnut shell.

The Freundlich isotherm model (FIG. 6.) also fitted the experimental data. However, the level of fitness was less as compared to that of the Langmuir model as indicated by a correlation coefficient of 0.9098. TABLE 15 showed that the value of n was found to be 1.631 indicating that the groundnut shell had a heterogeneous surface since the value satisfied the heterogeneity condition, that is $1 < n < 10$. In addition, the value of $\frac{1}{n}$ was below unity indicating a chemisorption process. The values of K_F were found to be small implying that there was low uptake of the metal ions unto the adsorbent surface. Comparing the models investigated, the Langmuir model showed the best representation of the equilibrium data than the Freundlich model indicating monolayer adsorption [36,37]. From literature, other studies also reported similar findings.

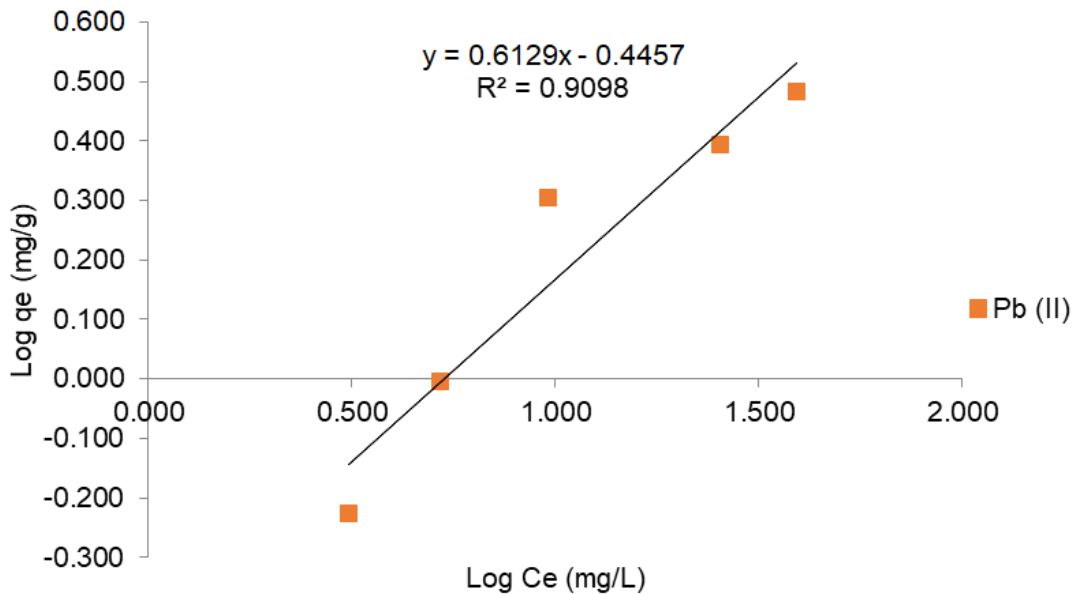


FIG. 5. Freundlich isotherm plot of Pb (II) ion onto groundnut shell.

Ogunleye et al., [57] used activated carbon produced from banana stalk for the removal of Pb (II). Four isotherm models, Langmuir, Freundlich, Tempkin and Dubini-Radushkevich models were employed in the equilibrium studies of the adsorption data. The results obtained from the study showed that the Langmuir model was the best-fitted model amongst the four models considered. Misihairabgwi et al., [58] studied on the adsorption of heavy metals using agroforestry waste derived activated carbon on solutions containing the metals. The metals considered were Pb (II), Hg (II), Fe (II), Cu (II), Zn (II), Ni (II), Cd (II), Mn (II), Cr (II) and As (II). The activated carbon was prepared from Macadamia nut shells, baobab shells, pigeon pea husk, rice husk, Moringa oleifera husks, and marula stones. It was found that the adsorption of these metals fitted the Langmuir model.

Adsorption equilibrium kinetic studies

The kinetic study determines the degree of utilization of the adsorption capacity as a function of the time of contact between the liquid and the solid. The kinetics of adsorption was determined by analyzing adsorptive uptake of the Pb (II) ions from the aqueous solution at different time intervals (10-240 min) while keeping other parameters constant. From the experimental data obtained from the kinetic experiment, the pseudo-first-order and pseudo-second-order were tested to determine the mechanisms of adsorption of Pb (II) ions onto the groundnut shell. The linear plots of the kinetic models are given in **FIG. 7**. while the calculated values of their constants and correlation coefficients (R^2) are summarized in **TABLE 16**.

TABLE 16. Calculated values of the various kinetic models' constants and their correlation coefficients (R^2) for the adsorption of Pb (II) ions onto groundnut shell.

Pseudo-first-order			Pseudo-second-order		
K_{p1} (L/min)	q_e (mg/g)	R^2	K_{p2} (L/min)	q_e (mg/g)	R^2
0.05	2.464	0.9819	0.004	4.464	0.9996

The plots of pseudo-first-order and pseudo-second-order models showed that the adsorption of Pb (II) onto the groundnut shell followed both the pseudo-first-order and pseudo-second-order models with good correlation coefficients as shown in **FIG. 7**. However, it was observed from **FIG. 7**. that the pseudo-second-order kinetic model of Pb (II) showed excellent linearity with high correlation coefficients $R^2 > 0.999$ in comparison to the pseudo-second-order model; hence, the best fit. In **TABLE 16**, the high values of the adsorption capacities (q_e) and rate constants of the pseudo-second-order (K_{p2}) kinetic model confirmed the agreement of experimental data with the pseudo-second-order model.

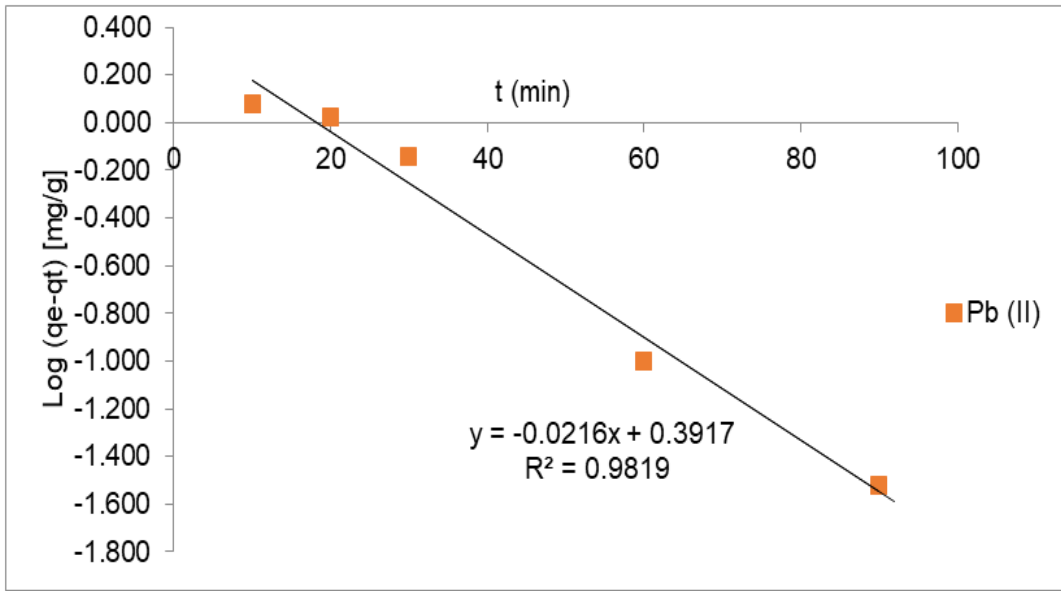


FIG. 6. Pseudo-First-order plot of Pb (II) ion onto groundnut shell.

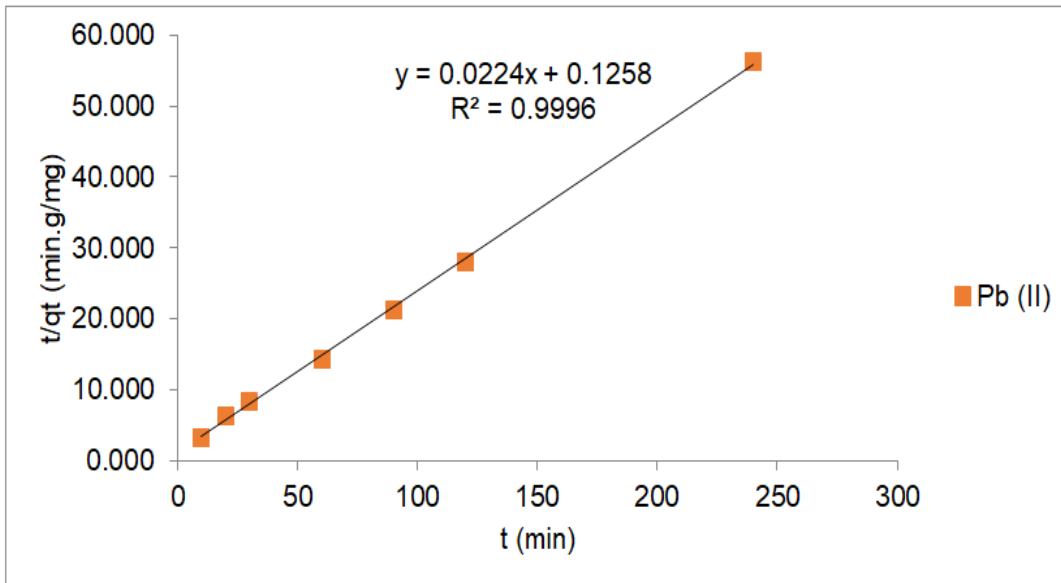


FIG. 7. Pseudo-Second-order plot of Pb (II) ion onto groundnut shell.

The best-fitted pseudo-second-order model explained the mechanism of Pb (II) biosorption onto the groundnut shell to be chemisorption process [2] where the metal ions stick to the adsorbent surface by forming a chemical (usually covalent) bond and tend to find sites that maximize their coordination number with the surface [59].

The fitness of Pb (II) experimental data to the pseudo-second-order was also in agreement with other studies. Bhattacharyya and Sharma [60] studied on the adsorption of Pb (II) from wastewater using mature neem (*Azadirachta indica*) leaves. The first-order and second-order kinetic models were used to explain the adsorption mechanism, but the adsorptive performance corresponded to pseudo-second-order model. Wong et al., [59] analyzed the removal of Pb (II) by means of a batch experiment using rice husk modified with tartaric acid. It was found that the pseudo-second-order model interpreted the

kinetics of reaction better than the pseudo-first-order model with evidence of high correlation coefficient. Similarly, Yahaya and Akinlabi, [61] made use of cocoa pod husk for the removal of Pb (II) and the kinetic studies best fitted into the pseudo-second-order model with the high R^2 a value ranging from 0.9776 to 1.

Conclusion

The optimization of Pb (II) adsorption from aqueous solution by the groundnut shell showed that the contact time, pH and initial Pb (II) concentration had a significant influence on removal efficiency and adsorption capacity of Pb (II). This was revealed by RSM where the interaction among the variables studied enhanced the adsorption of Pb (II). Applying the CCD under RSM, the optimized contact time (90 min), pH (8) and initial concentration (75 mg/L) of Pb (II) gave a maximum uptake of 90.26 % and adsorption capacity of 3.428 mg/g with the desirability of 0.966.

Langmuir isotherm model provided the best fit to the equilibrium data indicating that the adsorption of Pb (II) by the adsorbent (groundnut shell) was monolayer with homogeneous adsorption sites. The adsorption process followed the pseudo-second-order kinetic model thereby describing the mechanism of Pb (II) bio-sorption onto groundnut shell as a chemisorption process. The FT-IR analysis of the groundnut shell indicated that hydroxyl, carboxyl and amine groups were present while the SEM analysis revealed large pores on the biomass surface that could enhance the uptake of Pb (II). In this study, it could be concluded that the groundnut shell exhibited high potential for the removal of Pb (II) ions from aqueous media.

Conflict of Interest

The authors report no conflict of interest.

Acknowledgment

The authors appreciate the effort of the management of the University for Development Studies for equipping the Applied Chemistry and Biochemistry laboratory for core teaching and research work where this research work was carried out.

REFERENCES

1. Mohammad YS, Shaibu-Imodagbe EM, Igboro SB, et al. Modeling and optimization for production of rice husk activated carbon and adsorption of phenol. *J Eng.* 2014.
2. Samuel S, Abigail M, and Chidambaram R. Isotherm modeling, kinetic study, and optimization of batch parameters using response surface methodology for effective removal of Cr (VI) using fungal biomass. *PloS one.* 2015;10(3):e0116884.
3. Tsoi MF, Cheung CL, Cheung TT, et al. Continual decrease in blood lead level in Americans: United States National Health Nutrition and examination survey 1999-2014. *Am J Med.* 2016;129(11):1213-8.
4. Hara A, Thijs L, Asayama K, et al. Blood pressure in relation to environmental lead exposure in the national health and nutrition examination survey from 2003 to 2010. *Hypertension.* 2014:114.
5. McWeeny DJ. Toxic substances in crop plants, food, and chemical toxicology. The Royal Society of Chemistry, London.1993;31(2):149.
6. Wuana RA, Okieimen FE. Heavy metals in contaminated soils: A review of sources, chemistry, risks and best available strategies for remediation. *Isrn Ecology.* 2011.

7. Hardy DH, Myers J, Stokes CE. Heavy metals in North Carolina soils: Occurrence and significance. NC Department of Agriculture and Consumer Services, Agronomic Division; 2008.
8. V Asio, "Soil and Environment : Heavy metals in the environment and their health effects," Soil Environ. 2009.
9. Meunier N, Drogui P, Montané C, et al. Comparison between electrocoagulation and chemical precipitation for metals removal from acidic soil leachate. *J Hazard Mater.* 2006;137(1):581-90.
10. Eccles H. Treatment of metal-contaminated wastes: Why select a biological process? *Trends Biotechnol.* 1999;17(12):462-5.
11. Wu D, Niu C, Li D, et al. Solvent extraction of scandium(III), yttrium(III), lanthanum(III) and gadolinium(III) using Cyanex 302 in heptane from hydrochloric acid solutions. *J Alloys Compd.* 2004;374(1-2):442-6.
12. Garcia-Sánchez A, Alvarez-Ayuso E. Sorption of Zn, Cd, and Cr on calcite. Application to the purification of industrial wastewaters. *Miner Eng.* 2002;15(7):539-47.
13. Chen X. Modeling of experimental adsorption isotherm data. *Information.* 2015;6(1):14-22.
14. Shah BA, Shah AV, Singh RR. Sorption isotherms and kinetics of chromium uptake from wastewater using natural sorbent material. *Int J Environ Sci and Technol.* 2009;6(1):77-90.
15. Rahmani K, Mahvi AH, Vaezi F, et al. Bioremoval of lead by use of waste activated sludge. *Int J Environ Sci and Technol.* 2009;3(3):471-76
16. Edokpayi JN, Odiyo JO, Msagati TA, et al. A Novel Approach for the removal of lead(II) ion from wastewater using mucilaginous leaves of *diceriocaryum eriocarpum* plant. *Sustainability.* 2015;7(10):14026-41.
17. Kumari P, Sharma P, Srivastava S, et al. Biosorption studies on shelled *Moringa oleifera* Lamarck seed powder: removal and recovery of arsenic from aqueous system. *Int J Miner Process.* 2006;78(3):131-9.
18. Oboh OI, Aluyor EO. The removal of heavy metal ions from aqueous solutions using sour sop seeds as biosorbent. *Afr J Biotechnol.* 2008;7(24).
19. Li X, Tang Y, Cao X, et al. Preparation and evaluation of orange peel cellulose adsorbents for effective removal of cadmium, zinc, cobalt, and nickel. *Colloids and Surfaces A: Physicochemical and Engineering Aspects.* 2008;317(1-3):512-21.
20. Idris S, Iyaka YA, Dauda BE, et al. Kinetic study of utilizing groundnut shell as an adsorbent in removing chromium and nickel from dye effluent. *Am Chem Sci J.* 2012;2(1):12-24.
21. Khataee AR. Optimization of UV- promoted peroxydisulphate oxidation of CI Basic Blue 3 using response surface methodology. *Environ Technol.* 2010;31(1):73-86.
22. Xin-hui D, Srinivasakannan C, Qu WW, et al. Regeneration of microwave assisted spent activated carbon: process optimization, adsorption isotherms, and kinetics. *Chemical Engineering and Processing: Process Intensification.* 2012;53:53-62.
23. Abdel-Tawwab M, El-Sayed GO, et al. Capability of some agricultural wastes for removing some heavy metals from polluted water stocked in combination with Nile tilapia, *Oreochromis niloticus* (L.). *International Aquatic Research.* 2017;9(2):153-60.
24. Choudhury TR, Pathan KM, Amin MN, et al. Adsorption of Cr(III) from aqueous solution by groundnut shell. *J Environ Sci Water Res.* 2012;1(6):144-50.
25. APHA, APHA-Standard method for the examination of water and wastewater. Washington, DC: American Water Works Association and Water Pollution; Control Federation, 1989.

26. Bayuo J, Abukari MA, Pelig-Ba K.B, et al. Equilibrium isotherm studies for the sorption of hexavalent chromium (VI) onto groundnut shell. IOSR J. Appl. Chem. 2019;11(12):40–46.
27. Garba ZN, Bello I, Galadima A, et al. Optimization of adsorption conditions using a central composite design for the removal of copper(II) and lead(II) by defatted papaya seed. Karbala International Journal of Modern Science. 2016;2(1):20-8.
28. Sarrai AE, Hanini S, Merzouk NK, et al. Using central composite experimental design to optimize the degradation of tylosin from aqueous solution by the photo-Fenton reaction. Materials. 2016;9(6):428.
29. Mourabet M, El Rhilassi A, El Boujaady H, et al. Use of response surface methodology for optimization of fluoride adsorption in an aqueous solution by Brushite. Arab J Chem. 2017;10: S3292-302.
30. Owolabi RU, Usman MA, Kehinde AJ. Modeling and optimization of process variables for the solution polymerization of styrene using response surface methodology. J King Saud Univ. 2018;30(1):22-30.
31. Auta M. Optimization of tea waste activated carbon preparation parameters for removal of cibacron yellow dye from textile wastewaters. Int J Adv Res Technol. 2012;1(4):50-6.
32. Roy P, Mondal NK, Das K. Modeling of the adsorptive removal of arsenic: A statistical approach. J Environ Chem Eng. 2014;2(1):585-97.
33. Chattoraj S, Mondal NK, Das B, et al. Biosorption of carbaryl from aqueous solution onto Pistia stratiotes biomass. Appl Water Sci. 2014;4(1):79-88.
34. Langmuir I. The constitution and fundamental properties of solids and liquids. Part I. Solids. J Am Chem Soc. 1916;38(11):2221-95.
35. Freundlich HMF, Over the adsorption in solution. J Phys Chem. 1906;57:385-471.
36. Foo KY, Hameed BH. Insights into the modeling of adsorption isotherm systems. Chem Eng J. 2010;156(1):2-10.
37. Ghiaci M, Abbaspur A, Kia R, et al. Equilibrium isotherm studies for the sorption of benzene, toluene, and phenol onto organo-zeolites and as-synthesized MCM-41. Sep Purif Technol. 2004;40(3):217-29.
38. Chakravarty P, Sarma NS, Sarma HP. Removal of lead(II) from aqueous solution using heartwood of Areca catechu powder. Desalination. 2010;256(1-3):16-21.
39. Kumar KV, Sivanesan S. Sorption isotherm for safranin onto rice husk: Comparison of linear and non-linear methods. Dyes and Pigments. 2007;72(1):130-3
40. Haghseresht F, Lu GQ. Adsorption characteristics of phenolic compounds onto coal-reject-derived adsorbents. Energy and Fuels. 1998;12(6):1100-7.
41. Brasquet C, Subrenat E, Le Cloirec P. Selective adsorption on fibrous activated carbon of organics from aqueous solution: correlation between adsorption and molecular structure. Water Sci Technol. 1997;35(7):251-9.
42. Abas SN, Ismail MH, Kamal ML, et al Adsorption process of heavy metals by low-cost adsorbent: a review. World Applied Sciences Journal. 2013;28(11):1518-30.
43. Ho YS. Review of second-order models for adsorption systems. J Hazard Mater. 2006;136(3):681-9.
44. Aksu Z, Tezer S. Biosorption of reactive dyes on the green alga *Chlorella vulgaris*. Process Biochem. 2005;40(3-4):1347-61.
45. Inbaraj BS, Chien JT, Ho GH, et al. Equilibrium and kinetic studies on sorption of basic dyes by a natural biopolymer poly (γ -glutamic acid). Biochem Eng J. 2006;31(3):204-15.

46. Lagergren SK. About the theory of so-called adsorption of soluble substances. *Sven. Vetenskapsakad. Handlingar*. 1898;24:1-39.
47. Hameed BH, El- Khaiary MI. Batch removal of malachite green from aqueous solutions by adsorption on oil palm trunk fiber: equilibrium isotherms and kinetic studies. *J Hazard Mater*. 2008;154(1-3):237-44.
48. Hameed BH, El-Khaiary MI. Sorption kinetics and isotherm studies of a cationic dye using agricultural waste: Broad bean peels. *J Hazard Mater*. 2008;154(1-3):639-48.
49. Anirudhan TS, Radhakrishnan PG. Thermodynamics and kinetics of adsorption of Cu(II) from aqueous solutions onto a new cation exchanger derived from tamarind fruit shell. *J Chem Thermodyn*. 2008;40(4):702-9
50. Cheng W, Wang SG, Lu L, et al. Removal of malachite green (MG) from aqueous solutions by native and heat-treated anaerobic granular sludge. *Biochem Eng J*. 2008;39(3):538-46.
51. Hameed B. Equilibrium and kinetic studies of methyl violet sorption by agricultural waste. *J Hazard Mater*. 2008;154(1-3):204-12.
52. Al-Asheh S, Banat F, Masad A. Kinetics and equilibrium sorption studies of 4-nitrophenol on pyrolyzed and activated oil shale residue. *Environ Geol*. 2004;45(8):1109-17.
53. Yusuff AS. Optimization of adsorption of Cr(VI) from aqueous solution by *Leucaena leucocephala* seed shell activated carbon using the design of the experiment. *Appl Water Sci*. 2018;8(8):232.
54. Chaudhary N, Balomajumder C. Optimization study of adsorption parameters for removal of phenol on aluminum impregnated fly ash using response surface methodology. *J Taiwan Inst Chem Eng*. 2014;45(3):852-9.
55. Alam MZ, Ameen ES, Muyibi SA, et al. The factors affecting the performance of activated carbon prepared from oil palm empty fruit bunches for adsorption of phenol. *Chem Eng J*. 2009;155(1-2):191-8.
56. Rai A, Mohanty B, Bhargava R. Supercritical extraction of sunflower oil: A central composite design for extraction variables. *Food Chem*. 2016;192:647-59.
57. Ogunleye OO, Ajala MA, Agarry SE. Evaluation of biosorptive capacity of banana (*Musa paradisiaca*) stalks for lead (II) removal from aqueous solution. *J Environ Prot*. 2014;5(15):1451.
58. Misihairabgwi JM, Kasiyamhuru A, Anderson P, et al. Adsorption of heavy metals by agroforestry waste derived activated carbons applied to aqueous solutions. *Afr J Biotechnol*. 2014;13(14):1579-87
59. Wong KK, Lee CK, Low KS, et al. Removal of Cu and Pb by tartaric acid modified rice husk from aqueous solutions. *Chemosphere*. 2003;50(1):23-8.
60. Bhattacharyya KG, Sharma A. *Azadirachta indica* leaf powder as an effective biosorbent for dyes: A case study with aqueous Congo Red solutions. *J Environ Manage*. 2004;71(3):217-29.
61. Yahaya LE, Akinlabi AK. Equilibrium sorption of Lead(II) in aqueous solution onto EDTA-modified Cocoa (*Theobroma cacao*) Pod husk residue. *Iran J Energy Environ*. 2016;7:58-63.